

The model for the magnetization of current carrying amorphous ferromagnets

Sabolek, Stjepan

Source / Izvornik: **Fizika A, 1993, 2, 101 - 110**

Journal article, Published version

Rad u časopisu, Objavljena verzija rada (izdavačev PDF)

Permanent link / Trajna poveznica: <https://um.nsk.hr/um:nbn:hr:217:031745>

Rights / Prava: [In copyright](#)/[Zaštićeno autorskim pravom.](#)

Download date / Datum preuzimanja: **2024-09-11**



Repository / Repozitorij:

[Repository of the Faculty of Science - University of Zagreb](#)



THE MODEL FOR THE MAGNETIZATION OF CURRENT CARRYING
AMORPHOUS FERROMAGNETS

STJEPAN SABOLEK

Department of Physics, Faculty of Science, POBox 162, 41000 Zagreb, Croatia

Received 19 July 1993

UDC 538.955

Original scientific paper

A recent model for the explanation of the decrease of coercive field H_c and the core loss E in amorphous ribbons carrying a direct current J_d has been extended in order to account for the effects of an alternating core current J . The model predicts a linear decrease of H_c with the amplitude J_0 of J and the achievement of $H_c = 0$ for J_0 which is sufficient in order to release the domain walls responsible for H_c in the absence of the drive field H . The actual shape and frequency of the core current pulses appear to be immaterial as long as the condition $J = J_0$ at $H = 0$ is fulfilled. The accurate measurements performed on the stress-free $\text{Co}_{70.3}\text{Fe}_{4.7}\text{Si}_{15}\text{B}_{10}$ and twisted $\text{Fe}_{80}\text{B}_{20}$ ribbons confirm the validity of the model. Some applications of the phenomenon are briefly discussed.

1. Introduction

The earlier investigations have shown that a direct current J_d flowing along an amorphous ferromagnetic ribbon affects its process of magnetization [1-2]. In particular J_d shifts, broadens and decreases the maxima on its dM/dT vs. H curve. This results in M-H loop which is narrower (of a lower coercive field H_c) and slanted (of a lower maximum permeability) than that obtained in the absence of J_d . Usually J_d also shifts the center (C) of the M-H loop [3-4]. It has been shown [3-5] that

these effects are caused by the self-field of J_d which at the surfaces of a thin ribbon has the magnitude $H_p = J_d/2w$ (w is the width of the ribbon). Indeed, the surface fields H_p obtained from the external sources [6-7] produced the same effects on the M-H loops of amorphous ribbons as J_d . Accordingly, the effects of J_d on the M-H loops of amorphous ribbons have been attributed to the simultaneous influence of the drive field H and H_p on the movement of the domain walls (DW) responsible for H_c .

Recent calculation [8] of the variations of H_c and C with H_p for a hypotetic ribbon consisting of two domains with antiparallel magnetizations I forming a small angle δ with the ribbon axis confirmed the validity of the above approach. In particular, the calculated variations of H_c and C with H_p agreed quite well with those observed at lower magnitudes of H_p in the nonmagnetostrictive $\text{Co}_{70.3}\text{Fe}_{4.7}\text{Si}_{15}\text{B}_{10}$ (hereafter CoFeSiB) amorphous alloy. However, at the elevated H_p the observed variations deviated strongly from the calculated ones. Whereas the calculation predicted a linear decrease of H_c with H_p and constant C , the observed H_c tended to saturation and C showed an anomalous increase with H_p . This discrepancy was ascribed to the effects of the elevated H_p on the actual domain structure and the pinning of the DW in real sample. Therefore, it seems impossible to achieve the nonhysteretic M-H loop ($H_c = 0$) by means of J_d (or more generally static H_p) in the real amorphous ribbons.

Very recently [9] it was realized that a large increase of C at the elevated H_p can be employed in order to achieve $H_c = 0$ by means of an alternating core current J . Here we extend the calculations of Ref. 8 in order to account for an arbitrary δ and an alternating core current. A rather general condition for the occurrence of $H_c = 0$ by means of J is derived. The predictions of these calculations are verified by measuring the variations of H_c with dynamic $H_p(J)$ for the unstressed CoFeSiB and twisted $\text{Fe}_{80}\text{B}_{20}$ amorphous ribbons. The observed variations agree very well with the predicted ones.

2. Model and calculations

The model for the influence of core currents on the magnetization of the amorphous ferromagnetic ribbons takes into account the following observations:

- the main contribution to the magnetization of the as-quenched amorphous ribbon along its length comes from the stripe domains [10] separated with π -DW's,
- the magnetization I of a such domain forms in general an angle δ with the ribbon axis and this angle is not the same for all domains [11],
- at lower magnetizing fields H the magnetization of the ribbon occurs [12] through the movement of π -DW's,
- the strongest DW pinning centers are usually located at the surfaces of the ribbon and their strengths are generally different at the opposite surfaces [13].

Under these circumstances a useful simplification is to consider a ribbon consisting of two domains with magnetizations I separated with π -DW [5]. We label

the angle between I and the ribbon axis with δ and denote one surface of the ribbon as the “upper” and the opposite as the “lower”. Accordingly, the strengths of pinning of DW at the upper and lower surface of the ribbon are denoted with S_u and S_l , respectively. In order to be specific we assume $S_u < S_l$ and define the average pinning $\langle S \rangle = (S_u + S_l)/2$ and the pinning inhomogeneity $\Delta S = S_l - S_u$. Furthermore, we denote the magnetizing field H as “positive” when it increases from $-H_0$ to H_0 (H_0 is the amplitude of H) and “negative” when it decreases from H_0 to $-H_0$.

In the absence of the core current the magnetization changes when the projection of H on I , $P_{Hi} = H \cos \delta$ ($i = u, l$) reaches the value S_i which is required in order to release the DW from the particular surface of the sample. Since DW is first released from the surface with the lower pinning strength (the upper in our case) the coercive field will be $H_{c0} = S_u / \cos \delta$.

When direct current J_d flows along the ribbon, its self-field H_p exerts the pressure on DW, too. H_p lies in the plane of the ribbon and has the opposite directions (H_{pu} and H_{pl} in the inset to Fig. 2) at the opposite surfaces of the ribbon. We denote the projections of H_p on I by $P = H_{pi} \sin \delta$. Under these conditions P_{Hi} 's required to release DW for the “positive” H are [8]:

$$P_{Hu} = S_u \mp P \tag{1}$$

$$P_{Hl} = S_l \pm P. \tag{2}$$

For the “negative” H one has:

$$P_{-Hu} = -S_u \mp P \tag{3}$$

$$P_{-Hl} = -S_l \pm P. \tag{4}$$

In Eqs. (1)–(4) the upper signs of P corresponds to the directions of H_{pu} and H_{pl} shown in the inset to Fig. 2. Conversely, lower signs corresponds to the opposite direction of J_d . The variations of P_{Hi} 's and P_{-Hi} 's with P (assuming constant S_u and S_l) were illustrated in Fig. 1 in Ref. 8. Since the magnetization changes as soon as the projection of H on I reaches the lowest value required in order to unpin DW in the given circumstances (the direction of H , the directions and magnitudes of H_{pi} 's) only parts of the relations for P_{Hi} 's and P_{-Hi} 's will be relevant for the determination of the width (H_c) and the center (C) of the M-H loop. Accordingly [8] the variations of H_c and C with P will depend on the magnitude of P . In particular for $|P| \leq \Delta S/2$ is $|P_{Hu}| < |P_{Hl}|$ (Eqs. (1) and (2)) and $|P_{-Hu}| < |P_{-Hl}|$ (Eqs. (3) and (4)) for both signs of P . Therefore:

$$H_c = (P_{Hu} - P_{-Hu})/2 \cos \delta = S_u / \cos \delta \tag{5}$$

and

$$C = (P_{Hu} + P_{-Hu})/2 \cos \delta = \mp P / \cos \delta. \tag{6}$$

Analogously for $P > \Delta S/2$ is $|P_{Hu}| < |P_{Hl}|$ and $|P_{-Hl}| < |P_{-Hu}|$, hence:

$$H_c = (\langle S \rangle - P) / \cos \delta \tag{7}$$

and

$$C = -\Delta S/2 \cos \delta. \tag{8}$$

For the opposite direction of J_d is $|P_{Hl}| < |P_{Hu}|$ and $|P_{-Hu}| < |P_{-Hl}|$. This changes the sign of C in Eq. (8) but leaves Eq. (7) unchanged. Apparently the expressions (5)–(8) which are valid for an arbitrary angle δ coincide with Eqs. (5)–(8) in Ref. 8 when δ is a small angle ($\cos \delta \approx 1$). Furthermore since δ is constant in a given case the variations of H_c and C with P shown in Fig. 1 in Ref. 9 are qualitatively the same as those predicted by Eqs. (5)–(8).

We now consider the case when an alternating core current J flows along the ribbon. The simplest situation occurs when J has a rectangular waveform and the same frequency as H . For such J with the phase in respect to H shown in the inset in Fig. 1 P_{Hi} 's required in order to release DW are obtained by simple combining the relations (1)–(4) for both directions of J_d (signs of P). One obtains

$$P_{Hu} = S_u - P \tag{9}$$

$$P_{Hl} = S_l + P \tag{10}$$

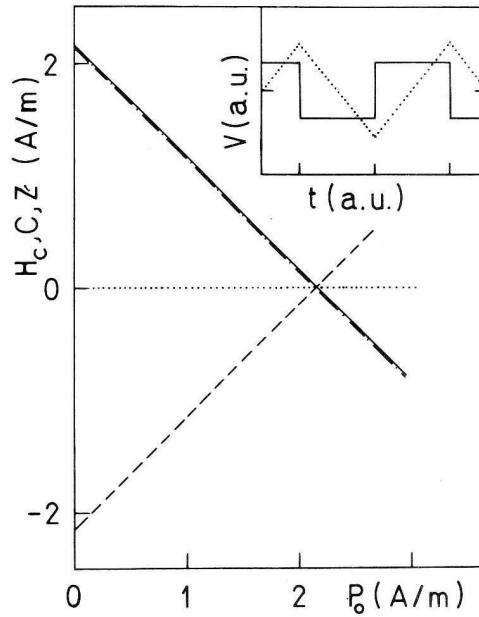


Fig. 1. Calculated coercive field H_c (---), center of the M-H loop C (···) and corresponding projections (Z) of driving field H for “positive” (–) and “negative” (– · –) H (see text) vs. projection P_0 of the field H_{p0} caused by rectangular current flowing along the “two-domain” ribbon. The inset: phase relationship between the drive field H (···) and rectangular core current (–).

for “positive” H , and

$$P_{-Hu} = -S_u + P \quad (11)$$

$$P_{-Hl} = -S_l - P \quad (12)$$

for “negative” H . Since $|P_{Hu}| < |P_{Hl}|$ and $|P_{-Hu}| < |P_{-Hl}|$

$$H_c = (S_u - P) / \cos \delta \quad (13)$$

and

$$C = 0 \quad (14)$$

irrespective of the magnitude of P . The corresponding variations of P_{Hi} 's, H_c and C with P (caused with the rectangular core current J) are shown in Fig. 1. The parameters H_{c0} and δ (hence P) were adjusted according to the experimental results obtained with direct core current J_d at low H_p for CoFeSiB alloy [8]. Evidently, for constant S_u , H_c decreases linearly with P and reaches zero value for $P = S_u = H_{c0} \cos \delta$ (Eq. (13)). We note that when using J_d (Eq. (7)) $H_c = 0$ is expected for $P = \langle S \rangle$. Since $\langle S \rangle > H_{c0} \cos \delta$ the use of J instead of J_d is advantageous. Furthermore in a case of J , H_c is insensitive to S_l , hence an anomalous increase in C (hence ΔS and S_l) at the elevated H_p which prevented the achievement of $H_c = 0$ by the use of J_d in the CoFeSiB alloy [8] should not affect the decrease of H_c with $P(J)$ for the same alloy. Comparing the condition for the achievement of $H_c = 0$ (Eq. (13)), $P = S_u$, with either Eq. (6) or (7) and (8) one finds that $H_c = 0$ is obtained for the amplitude of J equal to J_d for which $|C| = H_{c0}$. Therefore the achievement of $H_c = 0$ by means of J depends whether the shift of the M-H loop C equal to H_{c0} can be achieved by means of J_d or not. We note that the conditions which are detrimental for the reduction of H_c by means of J_d [8] facilitate the achievement of $H_c = 0$ by means of J .

The physical meaning of Eqs. (13) and (14) is very simple. They simply state that $H_c = 0$ is achieved when $P(J)$ is sufficiently large in order to unpin DW's responsible for H_c without the help of H ($H = 0$). Because of this the use of rectangular J is not necessary in order to achieve $H_c = 0$. Indeed any waveform of J which enables one to achieve $P = S_u$ at $H = 0$ can produce $H_c = 0$ [9]. Moreover $H_c = 0$ can also be achieved when the frequency of J is an odd multiple of that of H providing that the phases of J and H are properly adjusted [9].

For $P > S_u$, $H_c < 0$ follows (Fig. 1). This means that two branches of the M-H loop (those corresponding to “positive” and “negative” H , respectively) have exchanged their positions, i.e. an inverted M-H loop is obtained.

3. Experimental verification

The predictions of the model have been verified by measuring the variations of H_c and C with H_p (generated by J_d or J) for the stress-free nonmagnetostrictive

CoFeSiB alloy and twisted magnetostrictive $\text{Fe}_{80}\text{B}_{20}$ (thereafter FeB) alloy. The measurements of the M-H loops have been performed with an induction method [14] at room temperature. All the measurements were performed with the frequency 5.5 Hz [8]. The drive field amplitudes H_0 were 25 A/m and 100 A/m for the CoFeSiB and FeB sample, respectively. Two oscillators providing the alternating core current J and the drive field H were synchronized [9] in order to achieve the appropriate phase difference between H and $H_p(J)$. The frequency of J was the same as that of H . The rectangular and sinusoidal J have been used for CoFeSiB and FeB sample, respectively.

The variations of H_c and C with $H_p(J_d)$ for the stress-free FeB sample revealed that the pinning inhomogeneity ΔS is too small in order to achieve $C = H_{c0}$. Since a stress affects strongly both $\langle S \rangle$ and ΔS of the magnetostrictive alloys [2] the sample was twisted through 360° (the length of the sample was 20 cm) and the measurements performed under these conditions. The resulting variations of H_c and C with $H_p(J_d)$ are shown in Fig. 2.

For $H_p \leq 20$ A/m H_c is practically constant and C increases linearly with H_p (hence P) as predicted by the Eqs. (5) and (6). From the slope of C vs. H_p we deduced $\delta \approx 32^\circ$ for twisted FeB alloy. For $H_p > 20$ A/m

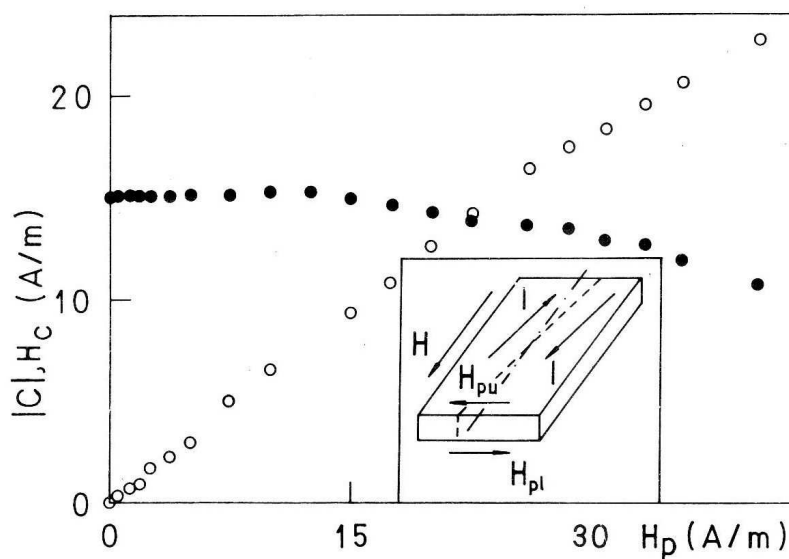


Fig. 2. Variation of the coercive field H_c (\bullet) and the center C (\circ) of the M-H loop with field H_p generated by the direct core current J_d flowing along the twisted $\text{Fe}_{80}\text{B}_{20}$ ribbon. The triangular drive field H with the amplitude $H_0 = 100$ A/m and frequency 5.5 Hz was used. The inset: Schematic drawing of the fields applied to the ribbon. I denotes the domain magnetizations, H_{pu} and H_{pl} are the fields induced by core current at the upper and lower surface of the sample, respectively.

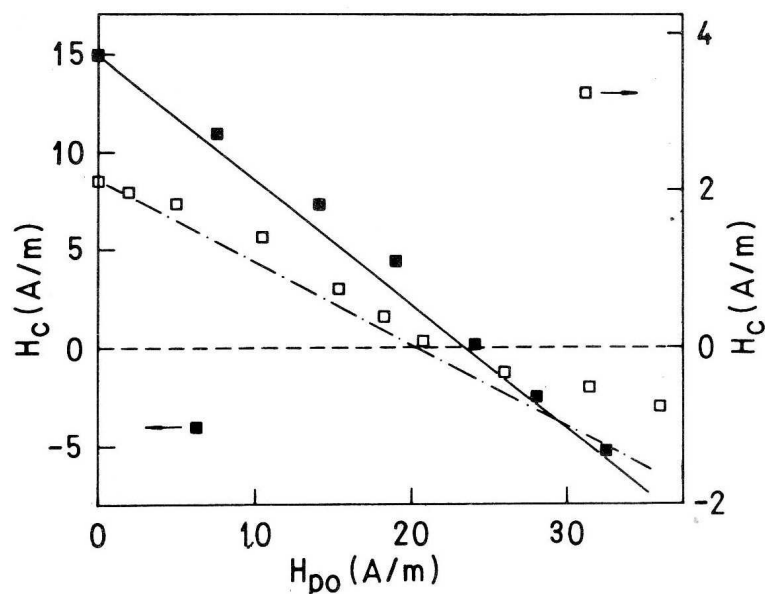


Fig. 3. The comparison of the observed (symbols) and calculated (lines) variations of the coercive field H_c with the projection P_0 of the field H_{p0} generated by the amplitude J_0 of the alternating core current J for $\text{Fe}_{80}\text{B}_{20}$ (\blacksquare) and $\text{Co}_{70.3}\text{Fe}_{4.7}\text{Si}_{15}\text{B}_{10}$ (\square) amorphous alloy. The measurements were performed at 5.5 Hz and the amplitudes of triangular drive field H were 100 A/m and 25 A/m for $\text{Fe}_{80}\text{B}_{20}$ and $\text{Co}_{70.3}\text{Fe}_{4.7}\text{Si}_{15}\text{B}_{10}$ alloy, respectively.

H_c decreases approximately linearly with H_p (Eq. (7)) but C continues to increase with H_p although at somewhat lower rate. The increase of C for $H_p > 20$ A/m indicates that ΔS increases with H_p at elevated H_p as was the case for CoFeSiB alloy [8]. This explanation is consistent with the rather slow decrease of H_c with H_p for $H_p > 20$ A/m (Fig. 2). Since at elevated H_p , $H_c \cos \delta = \langle S \rangle - P = S_u + \Delta S/2 - P$ the reduction of H_c due to sizable $P(\delta)$ is almost offset by the increase of ΔS for $H_p > 20$ A/m. We note that $C = H_{c0}$ is reached for $H_p \approx 23$ A/m which corresponds to $J_d \approx 92$ mA.

The results obtained with sinusoidal core current J flowing along the FeB sample are shown in Fig. 3. Here the calculated (Eqs. (13) and (14)) variations of H_c and C with H_{p0} ($H_{p0} = J_0/2w$, where J_0 is the amplitude of J) are shown. We note a very good agreement between the experimental results and the model predictions. In particular H_c reaches zero at about 23 A/m and becomes negative for $H_{p0} > 23$ A/m.

The variation of H_c and C with $H_p(J_d)$ for the stress-free CoFeSiB sample have been reported earlier [8] and will not be reported here. For this sample the observed variations of H_c and C with H_p deviated strongly from the model predictions at the

elevated values of H_p [8]. However C reached H_{c0} at about 22 A/m (corresponding to $J_d \approx 97$ mA).

The variations of H_c with $H_{p0}(J_0)$ for CoFeSiB sample is shown in Fig. 3. We note that the agreement between the calculated and observed variation for $H_{p0} \leq 22$ A/m is almost as good as that the twisted FeB sample. In particular H_c becomes zero at $H_{p0} = 22$ A/m. However for $H_{p0} > 22$ A/m H_c decreases less rapidly than expected. The comparison of the results obtained for J_d [8] with those presented here has shown that this occurs due to an increase of S_u with H_p which sets in for $H_p \geq 25$ A/m. [8,15] As for FeB sample $C \approx 0$ throughout the explored H_{p0} range has been obtained.

4. Conclusion

The calculations along the lines of a simple model for the influence of direct core current J_d on the M-H loops of amorphous ferromagnetic ribbons have been extended in order to account for effects of the alternating core currents J . Although the actual calculations were performed for a rectangular J having the same frequency as the magnetizing field H , the results obtained are valid for any waveform of J . Particularly, important result is a rather general condition for the occurrence of $H_c = 0$. This condition shows that $H_c = 0$ can be achieved by means of J whenever the shift C of M-H loop due to J_d can reach H_{c0} . Since C is associated with the pinning inhomogeneity ΔS and ΔS can be simply controlled (eg. with the application of the stress on the magnetostrictive alloy), it appears that $H_c = 0$ can be obtained by means of J in almost any ferromagnetic material. This was verified by comparing the calculated variations of H_c and C with $H_p(J)$ with those observed for the stress-free CoFeSiB and twisted FeB sample. In both cases the agreement between the model predictions and experimental results was very good. The reason that such a simple model explains so well the magnetization processes in amorphous ferromagnetic ribbons probably stems from a rather simple main domain structure of these materials [12]. The possibility to achieve $H_c = 0$ by means of J may be useful for the application in the cores of sensitive fluxgate magnetometers.

Acknowledgements

This work has been supported by NIST via funds made available through the scientific cooperation between Croatia and USA. Dr. H. H. Liebermann skillfully prepared the amorphous samples.

References

- 1) C. Aroca, E. Lopez and P. S. Sanchez, *J. Magn. Magn. Mater.* **23** (1981) 193;
- 2) R. N. G. Dalpadado, *IEEE Trans. Magn. MAG-17* (1981) 3163;
- 3) J. Horvat and E. Babić, *J. Magn. Magn. Mater.* **92** (1990) L25;
- 4) S. Sabolek, E. Babić and K. Zadro, *J. Magn. Magn. Mater.* **119** (1993) L10;
- 5) J. Horvat, E. Babić, Ž. Marohnić and H. H. Liebermann, *Philos. Mag.* **B63** (1991) 1235;
- 6) J. Horvat, E. Babić and G. J. Morgan, *J. Magn. Magn. Mater.* **104–107** (1992) 359;
- 7) S. Sabolek, J. Horvat, E. Babić and K. Zadro, *J. Magn. Magn. Mater.* **110** (1992) L25;
- 8) S. Sabolek, E. Babić and K. Zadro, *Fizika* **A1** (1992) 167;
- 9) S. Sabolek, E. Babić and Ž. Marohnić, *Philos. Mag. Lett.* **67** (1993) 399;
- 10) Y. Obi, H. Fujimori and H. Saito, *J. Appl. Phys.* **15** (1976) 611;
- 11) H. J. de Wit and M. Brouha, *J. Appl. Phys.* **57** (1985) 3560;
- 12) P. Schönhuber, H. Pfützner, G. Harasko, T. Klinger and K. Futschik, *J. Magn. Magn. Mater.* **112** (1992) 349;
- 13) J. Horvat and E. Babić, *J. Magn. Magn. Mater.* **96** (1991) 13 and references therein;
- 14) J. Horvat, Ž. Marohnić and E. Babić, *J. Magn. Magn. Mater.* **82** (1989) 5;
- 15) S. Sabolek, E. Babić and Ž. Marohnić, *Phys. Rev.* **B** (1993) in print.

MODEL MAGNETIZIRANJA AMORFNOG FEROMAGNETA KOJIM TEČE STRUJA

STJEPAN SABOLEK

*Fizički odjel, Prirodoslovno-matematički fakultet Sveučilišta u Zagrebu, Bijenička 32,
41000 Zagreb*

UDK 538.955

Orginalni znanstveni rad

Nedavno predloženi model za sniženje koercitivnog polja H_c i gubitaka energije u feromagnetskim trakama kojima teče istosmjerna struja J_d proširen je na izmjenične struje J . U slučaju izmjenične struje model predviđa linearno smanjenje H_c s amplitudom $J(J_0)$ te dostizanje $H_c = 0$ kod vrijednosti J_0 koja je dostatna da oslobodi domenske zidove koji su odgovorni za H_c u odsustvu magnetizirajućeg polja H . Sam oblik i frekvencija J su nevažni dotle dok je $J = J_0$ za $H = 0$ ispunjeno. Precizna mjerenja izvršena na nenapregnutoj $\text{Co}_{70.3}\text{Fe}_{4.7}\text{Si}_{15}\text{B}_{10}$ i tordiranoj $\text{Fe}_{80}\text{B}_{20}$ amorfnoj slitini potvrđuju valjanost modela. Ukratko su razmatrane neke primjene modela te posebno odsustva koercitivnog polja.